

# MEASURING $\Omega_M$ WITH THE ROSAT DEEP CLUSTER SURVEY

S. BORGANI<sup>1</sup>, P. ROSATI<sup>2</sup>, P. TOZZI<sup>3</sup>, S.A. STANFORD<sup>4</sup>, P.E. EISENHARDT<sup>5</sup>,  
C. LIDMAN<sup>2</sup>, B. HOLDEN<sup>4</sup>, R. DELLA CECA<sup>6</sup>, C. NORMAN<sup>7</sup> & G. SQUIRES<sup>8</sup>

<sup>1</sup> INFN, Sezione di Trieste, c/o Dipartimento di Astronomia dell'Università, via Tiepolo 11, I-34100 Trieste, Italy  
INFN, Sezione di Perugia, c/o Dipartimento di Fisica dell'Università, via A. Pascoli, I-06123 Perugia, Italy  
E-mail: borgani@ts.astro.it(borgani@ts.astro.it)

<sup>2</sup> ESO – European Southern Observatory, D-85748 Garching bei München, Germany  
E-mail: prosati@eso.org

<sup>3</sup> Osservatorio Astronomico di Trieste, via Tiepolo 11, I-34131 Trieste, Italy  
E-mail: tozzi@ts.astro.it

<sup>4</sup> Physics Department, University of California-Davis, Davis, CA 95616, USA  
Institute of Geophysics and Planetary Physics, Lawrence Livermore National Laboratory  
E-mail: adam@igpp.ucllnl.org, bholden@beowulf.ucllnl.org

<sup>5</sup> Jet Propulsion Laboratory, California Institute for Technology, MS 169-327, 4800 Oak Grove, Pasadena, CA 91109, USA  
E-mail: prme@kromos.jpl.nasa.gov

<sup>6</sup> Osservatorio Astronomico di Brera, via Brera 28, I-20121 Milano, Italy  
E-mail: rdc@brera.mi.astro.it

<sup>7</sup> Department of Physics and Astronomy, The Johns Hopkins University, Baltimore, MD 21218, USA  
E-mail: norman@stsci.edu

<sup>8</sup> Caltech Astronomy M/S 105-24, 1200 E. California Blvd., Pasadena, CA 91125, USA  
E-mail: gks@phobos.caltech.edu

## ABSTRACT

We analyze the ROSAT Deep Cluster Survey (RDCS) to derive cosmological constraints from the evolution of the cluster  $X$ -ray luminosity distribution. The sample contains 103 galaxy clusters out to  $z \simeq 0.85$  and flux-limit  $F_{lim} = 3 \times 10^{-14} \text{ erg s}^{-1} \text{ cm}^{-2}$  (RDCS-3) in the [0.5–2.0] keV energy band, with a high-redshift extension containing four clusters at  $0.90 \leq z \leq 1.26$  and brighter than  $F_{lim} = 1 \times 10^{-14} \text{ erg s}^{-1} \text{ cm}^{-2}$  (RDCS-1). We assume cosmological models to be specified by the matter density parameter  $\Omega_m$ , the r.m.s. fluctuation amplitude at the  $8 h^{-1} \text{ Mpc}$  scale  $\sigma_8$ , and the shape parameter for the CDM-like power spectrum  $\Gamma$ . Model predictions for the cluster mass function are converted into the  $X$ -ray luminosity function in two steps. First we convert mass into intra-cluster gas temperature by assuming hydrostatic equilibrium. Then temperature is converted into  $X$ -ray luminosity by using the most recent data on the  $L_X$ - $T_X$  relation for nearby and distant clusters. These include the Chandra data for seven distant clusters at  $0.57 \leq z \leq 1.27$ . From RDCS-3 we find  $\Omega_m = 0.35^{+0.13}_{-0.10}$  and  $\sigma_8 = 0.66^{+0.06}_{-0.05}$  for a spatially flat Universe with cosmological constant, with no significant constraint on  $\Gamma$  (errors correspond to  $1\sigma$  confidence levels for three fitting parameters). Even accounting for both theoretical and observational uncertainties in the mass- $X$ -ray luminosity conversion, an Einstein-de-Sitter model is always excluded at far more than the  $3\sigma$  level. We also show that the number of  $X$ -ray bright clusters in RDCS-1 at  $z > 0.9$  are expected from the evolution inferred at  $z < 0.9$  data. *Subject headings:*

Cosmology: theory - dark matter - galaxies: clusters: general - X-rays: galaxies

## 1 INTRODUCTION

According to the standard picture of hierarchical clustering, galaxy clusters arise from the gravitational collapse of exceptionally high peaks of the primordial density perturbations. Therefore, they probe the high-density tail of the distribution of the cosmic density field, usually assumed to be Gaussian, and their number density is exponentially sensitive to the cosmological scenario (e.g., White, Efstathiou & Frenk 1983). The low-redshift cluster abundance has been used over the last decade to measure the amplitude of density perturbations on  $\sim 10 h^{-1} \text{ Mpc}$  scales (here  $h$  is the Hubble constant in units of  $100 \text{ km s}^{-1} \text{ Mpc}^{-1}$ ), while the redshift evolution of the cluster abundance reflects the growth rate of density perturbations, i.e., primarily depends on the matter density parameter  $\Omega_m$  (e.g., Oukbir & Blanchard 1992; Eke et al. 1998). Al-

though very powerful in principle, this cosmological test faces two main problems in practical applications. First, theoretical predictions always provide the number density of clusters of a given mass, while the mass itself is never the directly observed quantity. Therefore, suitable assumptions are required to relate an observational quantity to the actual cluster mass. Secondly, a cluster sample is needed which spans a large  $z$ -baseline, and is based on model-independent selection criteria, so that the search volume and the number density associated with each cluster are uniquely specified. In this respect,  $X$ -ray observations provide a very efficient method to identify distant clusters down to a given  $X$ -ray flux limit, and hence within a known survey volume for each luminosity,  $L_X$ . For this reason, most of the studies which have used clusters as cosmological probes in the literature so far are based on

$X$ -ray selected samples. Following the pioneering work based on the Einstein Extended Medium Sensitivity Survey (EMSS, Gioia et al. 1990; Henry et al. 1992), deep imaging data from the ROSAT archive have been the basis for several serendipitous, flux-limited searches for high-redshift clusters (RDCS by Rosati et al. 1995, 1998; 160 deg<sup>2</sup> Survey by Vikhlinin et al. 1998; SHARC by Romer et al. 2000; WARPS by Jones et al. 1998; NEP by Gioia et al. 2001; see also Rosati et al. 2000 and Gioia 2000 for recent reviews).

Estimates of the  $X$ -ray temperature,  $T_X$ , for subsets of these samples have opened the way to measure cluster masses to a fairly good,  $\sim 15\%$ , precision (e.g., Evrard, Metzler & Navarro 1996). The resulting  $X$ -ray temperature functions (XTF) have been presented for both nearby (e.g., Henry & Arnaud 1991; Markevitch 1998; see Pierpaoli, Scott & White 2001, for a recent review) and distant clusters (e.g., Eke et al. 1998; Donahue & Voit 1999; Henry 2000), and have been compared with predictions from cosmological models. The mild evolution of the XTF has been interpreted as a strong indication for a low-density Universe, with  $0.2 \lesssim \Omega_m \lesssim 0.6$ . However, uncertainties related to the limited amount of high- $z$  data and to the lack of a homogeneous sample selection for local and distant clusters could substantially weaken this conclusion (Colafrancesco, Mazzotta & Vittorio 1997; Viana & Liddle 1999; Blanchard et al. 2000).

An alternative method to estimate cluster masses is based on applying the virial theorem to internal velocity dispersions,  $\sigma_v$ , as traced by redshifts of member galaxies. This method leads to a rather precise determination of the mass function of nearby clusters (Girardi et al. 1998), although it is observationally very time consuming. The only statistically well-defined sample of distant clusters where this method has been applied is the CNOC survey by Carlberg et al. (1997), which contains clusters selected from the EMSS. Even in this case, the limited size and redshift extension of CNOC did not allow to stringent constraints to be placed on  $\Omega_m$  from the distribution of cluster masses (Borgani et al. 1999b).

It is worth noting also that the analyses realized so far on the evolution of the XTF and of the  $\sigma_v$ -distribution combine samples of nearby and distant cluster, which have different selection criteria. In principle, this could complicate the comparison between low- and high-redshift data when establishing the evolution of the cluster population.

A further method to trace the evolution of the cluster number density is to follow the evolution of the  $X$ -ray luminosity function (XLF). The relation between the observed  $L_X$  and the cluster virial mass is affected by the thermodynamical status of the intra-cluster medium (ICM). Recent observations (Ponman, Cannon & Navarro 1999) show an excess entropy in the ICM, not explained by gravitational processes. This demonstrates that non-gravitational heating and, possibly, radiative cooling significantly affects the  $L_X$ - $M$  relation. Despite such complexities of the ICM physics, the  $X$ -ray luminosity has been shown to be a fairly robust diagnostic of cluster

masses (e.g., Borgani & Guzzo 2001). Furthermore, the most recent flux-limited cluster samples contain now a large ( $\sim 100$ ) number of objects, which are homogeneously identified over a broad redshift baseline, out to  $z \simeq 1.3$ . This provides a reliable way of combining data on nearby and distant clusters and a straightforward estimate of the selection function.

Kitayama & Suto (1997) and Mathiesen & Evrard (1998) analyzed the number counts from different  $X$ -ray flux-limited cluster surveys and found that resulting constraints on  $\Omega_m$  are rather sensitive to the evolution of the mass-luminosity relation. Sadat, Blanchard & Oukbir (1998) and Reichart et al. (1999) analyzed the EMSS and found results to be consistent with  $\Omega_m = 1$ . In our previous paper (Borgani et al. 1999, BRTN hereafter), we analyzed the XLF from the ROSAT Deep Cluster Survey (RDCS), as derived by Rosati et al. (1998) at different redshift intervals, from a cluster sample shallower than the one analyzed here (see Section 2.1, below). We were able to set only moderate constraints on the density parameter; we found  $\Omega_m \simeq 0.4 \pm 0.3$  (90% confidence level) for a non-evolving  $L_X$ - $T$  relation, with a critical-density model still allowed by a moderate positive evolution of this relation. The weakness of these constraints was partly due to the method of analysis, and partly to the smaller size of the analyzed sample. More recently, a consistent result has been also found by Evrard et al. (2001), who compared the RDCS redshift distribution to results from the Hubble volume simulations.

In this paper, we present the results on cosmological constraints from the analysis of the redshift and luminosity cluster distribution from the final version of the RDCS. This analysis differs from that in BRTN in several respects. First of all, the RDCS sample we analyze here is substantially enlarged (see Section 2.1), containing more than 100 clusters selected to a fainter flux limit and out to a larger redshift,  $z \lesssim 1.3$ . Furthermore, in BRTN we fitted the XLF after computing it within finite  $L_X$  and  $z$  intervals. The analysis presented in this paper, instead, is based on a maximum-likelihood method which does not rely on any binning of the data and, therefore, has the advantage of exploiting all the information contained in the cluster distribution within the whole portion of the  $(L_X, z)$  plane accessible to the RDCS. Finally, we base the luminosity-temperature conversion on the most recent observations, which probe now the whole redshift range sampled by RDCS clusters (e.g., Mushotzky & Scharf 1997; Donahue et al. 1999; Della Ceca et al. 2000), with the notable extension out to  $z \simeq 1.3$  from the Chandra observations of the ICM in the Lynx field (Stanford et al. 2001; Holden et al. 2001). We will devote particular care to verifying whether and by how much present uncertainties in the mass-luminosity relation weaken the derived constraints on the matter density parameter and on the amplitude of density perturbations at the cluster scale.

The plan of the paper is as follows. After briefly introducing the RDCS sample used for this analysis, we discuss the theoretical mass function and our approach to convert

observed  $X$ -ray fluxes into cluster masses. Finally, we describe in detail the maximum-likelihood method that we apply to derive constraints on cosmological parameters. In Section 3 we present the results of our analysis and we discuss the main conclusions in Section 4. Unless otherwise stated, unabsorbed fluxes and luminosities refer to the [0.5–2.0] keV energy band.

## 2 THE RDCS ANALYSIS

### 2.1 The sample

The RDCS sample was constructed from a serendipitous search for extended sources in ROSAT PSPC pointings with exposure longer than 15 ksec. A wavelet-based algorithm was used to detect and measure the angular extent of  $X$ -ray sources. Over 160 cluster candidates were selected in 180 PSPC fields as sources with an extent exceeding the local PSF with a 90% confidence level, which was statistically determined by a control sample of several thousands sources (Rosati et al. 1995, 1998).

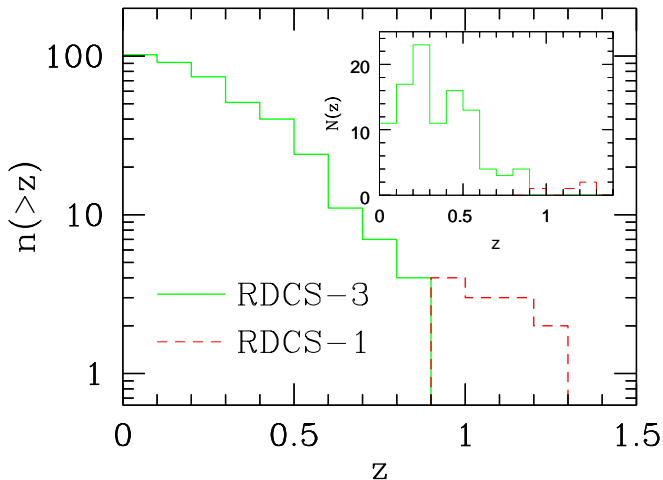


Fig. 1.—The cumulative redshift distribution,  $n(> z)$  of RDCS-3 clusters (continuous line) and of the high- $z$  extension of the RDCS-1 clusters (dashed line). Also shown in the insert plot is the differential redshift distribution,  $N(z)$ , for the same samples.

The RDCS sample that we consider in the following analysis is complete down to the flux limit  $F_{\text{lim}} = 3 \times 10^{-14} \text{ erg s}^{-1} \text{ cm}^{-2}$  (RDCS-3 hereafter) and contains 103 spectroscopically confirmed clusters at  $z \leq 0.85$  identified over an area of approximately  $50 \text{ deg}^2$ . This sample represents a substantial improvement with respect to that considered by BRTN, which included 70 clusters over an area of  $32 \text{ deg}^2$ , above a flux-limit of  $4 \times 10^{-14} \text{ erg s}^{-1} \text{ cm}^{-2}$ . In Figure 1 we show the cumulative and differential redshift distributions of the RDCS-3 clusters. RDCS-3 has overall a median redshift  $z_{\text{med}} = 0.29$ , with  $z_{\text{max}} = 0.85$ ; 26 clusters lie at  $z > 0.5$ , and 4 clusters at  $z > 0.8$ . Several other clusters with  $0.5 < z < 0.9$  have been identified in the RDCS at  $F_X < 3 \times 10^{-14} \text{ erg s}^{-1} \text{ cm}^{-2}$ ,

these, however, do not belong to a complete sample (see below) and hence are not included in the present analysis. The largest flux is  $F_{\text{max}} = 1.24 \times 10^{-12} \text{ erg s}^{-1} \text{ cm}^{-2}$ , with a median value of the flux distribution  $F_{\text{med}} = 9.9 \times 10^{-14} \text{ erg s}^{-1} \text{ cm}^{-2}$ . Further details about the sample, along with the presentation of the sky-coverage and an analysis of the XLF evolution are presented in a separate paper (Rosati et al., in preparation). In addition, we also consider a deeper subsample of four clusters identified down to  $F_{\text{lim}} = 1 \times 10^{-14} \text{ erg s}^{-1} \text{ cm}^{-2}$  in the redshift range  $0.90 \leq z \leq 1.26$  (RDCS-1 hereafter), whose  $z$ -distribution is also shown in Fig. 1. With the RDCS flux-limit and sky-coverage, we find, for a critical density Universe, that a cluster with  $L_X = 5 \times 10^{44} \text{ erg s}^{-1}$  has a searching volume  $V_{\text{max}} \simeq 4.5 \times 10^7 (h^{-1} \text{ Mpc})^3$  at  $z > 0.5$  and  $V_{\text{max}} \simeq 3.5 \times 10^7 (h^{-1} \text{ Mpc})^3$  for RDCS-3.

As discussed in Rosati et al. (1998), the sky-coverage and sample completeness become uncertain at fluxes  $\lesssim 3 \times 10^{-14} \text{ erg s}^{-1} \text{ cm}^{-2}$ . This is basically due to the fact that with  $\lesssim 50$  counts, which roughly correspond to the above flux for the typical exposure time of the selected PSPC fields, the detection and characterization of extended sources becomes increasingly uncertain. Furthermore, deep Chandra observations of the faintest RDCS clusters in the Lynx field (Stanford et al. 2001) show that, for such faint sources, PSPC-based  $X$ -ray fluxes can be significantly contaminated by emission from foreground or background point-like sources. For these reasons, we base our main analysis on the relatively bright sample, RDCS-3, while we will discuss whether the resulting constraints are consistent with the presence of the four clusters in the higher- $z$ , lower-flux tail. Overall, our analysis will draw information on the evolution of the cluster number density from the widest redshift baseline presently accessible with deep cluster surveys.

### 2.2 Modeling the $L_X$ distribution

Predictions for the  $L_X$ - and  $z$ -distributions of RDCS clusters are obtained by first computing the evolution of the cluster mass function and then by converting “theoretical” masses into observed  $X$ -ray fluxes (see also Kitayama & Suto 1997; BRTN).

The cluster mass function is usually written as  $n(M, z)dM = (\bar{\rho}/M)f(\nu)(d\nu/dM)dM$ , where  $\bar{\rho}$  is the cosmic mean density and  $\nu = \delta_c/\sigma_M(z)$ . Here  $\delta_c$  is the critical density contrast for top-hat halo collapse, extrapolated at the present time by linear theory ( $\delta_c = 1.686$  for  $\Omega_m = 1$ ), and  $\sigma_M(z)$  the r.m.s. value of a top-hat density fluctuation at the mass-scale  $M$  at redshift  $z$ . Recently, Sheth & Tormen (1999) have proposed for  $f(\nu)$  the expression

$$f(\nu) = \sqrt{\frac{2a}{\pi}} C \left( 1 + \frac{1}{(a\nu^2)^q} \right) \exp\left(-\frac{a\nu^2}{2}\right), \quad (1)$$

where  $a = 0.707$ ,  $C = 0.3222$  and  $q = 0.3$ , and showed that it provides a good fit to the halo mass function from N-body simulations (e.g., Governato et al. 1999; Jenkins et al. 2001). In the above equation the normalization is determined by the requirement  $\int f(\nu)d\nu = 1$ . Eq.(1) re-

duces to the standard Press–Schechter (1974) recipe for  $a = 1$ ,  $C = 1/2$  and  $q = 0$ . We assume each cosmological model to be specified by the matter density parameter,  $\Omega_m$ , and by the CDM-like power spectrum (Bardeen et al. 1986), with profile given by the shape–parameter  $\Gamma$  and normalization by the r.m.s. fluctuation amplitude within a sphere of  $8 h^{-1} \text{Mpc}$  comoving radius,  $\sigma_8$ . Unless otherwise specified, in the following we assume flat spatial geometry provided by a cosmological constant term,  $\Omega_\Lambda = 1 - \Omega_m$ , consistent with recent small scale measurements of CMB anisotropies (de Bernardis et al. 2000; Hanany et al. 2000). The value of  $\Omega_\Lambda$  is known to have a relatively small effect on the evolution of the mass function, and is far from being constrained by current cluster samples.

Comparing a theoretical mass function with the observed  $L_X$  distribution of the RDCS requires a suitable method to convert masses into  $X$ –ray luminosities in the appropriate energy band, [0.5–2.0] keV. As a first step we convert mass into temperature by assuming virialization, hydrostatic equilibrium, and isothermal gas distribution, according to the relation  $k_B T = 1.38 \beta^{-1} M_{15}^{2/3} [\Omega_m \Delta_{vir}(z)]^{1/3} (1+z)$  keV (e.g., Eke et al. 1998). Here we take 76% of the gas to be hydrogen,  $M_{15}$  is the cluster virial mass in units of  $10^{15} h^{-1} M_\odot$ ,  $\beta$  the ratio between the kinetic energy of dark matter and the gas thermal energy ( $\beta = 1$  would be expected for a perfectly thermalized gas) and  $\Delta_{vir}(z)$  the ratio between the average density within the virial radius and the mean cosmic density at redshift  $z$  ( $\Delta_{vir} = 18\pi^2 \simeq 178$  for  $\Omega_m = 1$ ). Although the assumptions on which the above relation is based have been recently questioned (e.g., Voit 2000), such a simple approach has been shown to reproduce fairly well the results from hydrodynamical cluster simulations (e.g., Bryan & Norman 1998, and references therein), with  $1 \lesssim \beta \lesssim 1.5$ . We assume for reference the value  $\beta = 1.15$  found by the Santa Barbara Cluster Comparison project (Frenk et al. 1999). We note that the  $M$ – $T_X$  relation can be affected by the thermodynamics of the ICM. For instance, in their model for non–gravitational gas heating, Tozzi & Norman (2001) predict masses which can differ by about 20–30% with respect to those obtained from the above  $M$ – $T$  relation. Possible deviations with respect to this relation are also indicated by observational data, when considering the mass within the internal cluster region at overdensity  $\delta > 500$  (Finoguenov, Reiprich & Böhringer 2001). Overall, we expect non–gravitational pre–heating to introduce fairly moderate changes in the  $M$ – $T_X$  relation used in our analysis. In order to account for them, in the following we will show the effect of changing  $\beta$  on the final model constraints. Finally, we assume 15% cluster-to-cluster scatter in converting temperature into mass, as suggested by numerical simulations (Metzler, Evrard & Navarro 1996).

As for the relation between temperature and bolometric

luminosity, we take the phenomenological expression

$$L_{bol} = L_6 \left( \frac{T_X}{6 \text{keV}} \right)^\alpha (1+z)^A \left( \frac{d_L(z)}{d_{L,EdS}(z)} \right)^2 10^{44} h^{-2} \text{erg s}^{-1}. \quad (2)$$

In this expression,  $L_6$  is a dimensionless quantity and  $d_L(z)$  the luminosity–distance at redshift  $z$  for a given cosmology, so that we explicitly factorize the redshift dependence induced by changing the spatial geometry of the cosmological background with respect to the Einstein–de–Sitter (EdS) model. Several independent analyses of nearby clusters with  $T_X \gtrsim 1$  keV consistently show that  $L_6 \simeq 3$  as rather stable results and  $\alpha \simeq 2.5$ – $3$  (e.g., White, Jones & Forman 1997; Wu, Xue & Fang 1999, and references therein), with a rather small scatter,  $\lesssim 30\%$ , especially once cooling flow effects are taken into account (e.g., Markevitch 1998; Allen & Fabian 1998; Arnaud & Evrard 1999). For cooler groups,  $\lesssim 1$  keV, the  $L_{bol}$ – $T_X$  relation steepen, with a slope  $\alpha \sim 5$  (e.g., Helsdon & Ponman 2000). As for the redshift evolution, Mushotzky & Scharf (1997) found that data out to  $z \simeq 0.4$  are consistent with no evolution for an EdS model (i.e.,  $A \simeq 0$ ), a result which is consistent also with more recent data on cluster temperatures out to  $z \simeq 0.8$  (Donahue et al. 1999; Della Ceca et al. 2000; Henry 2000).

In Table 1 we provide an update of the results available on temperature determinations of distant ( $z \geq 0.57$ ) clusters from recent Chandra observations. The two  $z > 1$  clusters (Stanford et al. 2001) and the  $z = 0.57$  cluster (Holden et al. 2001) have been observed in the Lynx field with 190 ksec ACIS-I exposure. The cluster CDFS-Cl1 has been detected as an extended source in the 1 Msec observation of the Chandra Deep Field South (Giacconi et al. 2001; Tozzi et al. 2001), its flux and temperature having been estimated from about 350 counts (further details are presented in Giacconi et al. in preparation). The cluster 1WGAJ1226.9 at  $z = 0.89$  has been serendipitously discovered in the WARPS by Ebeling et al. (2001) and, independently, by Cagnoni et al. (2001) in a ROSAT PSPC blank field. Its temperature has been measured by Cagnoni et al. with a 10 ksec ACIS-S observation. As for the cluster MS1137, it has been observed with a 120 ksec ACIS-S pointing. We analyzed the corresponding Chandra archival data by applying the same procedure described by Stanford et al. (2001). The bolometric luminosity quoted in Table 1 is computed within an aperture radius of  $60''$ . The resulting temperature,  $T = 5.7^{+0.8}_{-0.6}$  keV, turns out to be consistent with, although somewhat more precise than, that determined by Donahue et al. (1999) from ASCA data. Results for the cluster MS1054 have been obtained by Jeltama et al. (2001) from a 90 ksec exposure with Chandra ACIS-S. Also in this case, the temperature is consistent with, although slightly smaller than that based on ASCA observations.

The results for these distant clusters, along with other  $L_X$ – $T$  data for both distant and nearby clusters, are shown in Figure 2. Overall, the results reported here constrain the evolution of the  $L_{bol}$ – $T_X$  relation over the largest red-

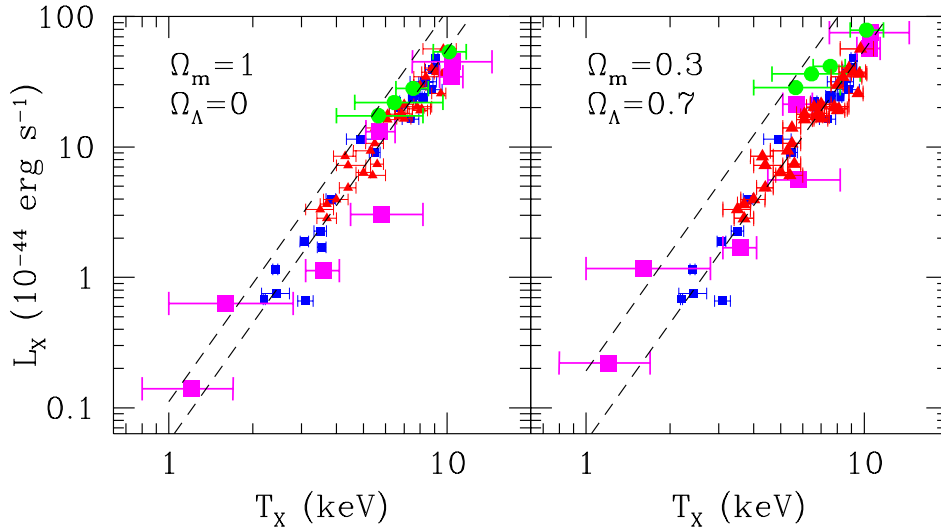


Fig. 2.— The luminosity–temperature relation for nearby and distant clusters in two different cosmologies. Values of  $L_X$  assume here  $h = 0.5$  for the Hubble parameter. The nearby clusters analyzed by Markevitch (1998) and by Arnaud & Evrard (1999) are indicated with small triangles and squares, respectively. Large circles are for the compilation of clusters at  $0.5 \lesssim z \lesssim 0.8$  reported by Della Ceca et al. (2000). The large squares are for the compilation of distant ( $0.57 \leq z \leq 1.27$ ) clusters recently observed with Chandra and reported in Table 1. The dashed lines indicate the  $L_{bol}$ – $T_X$  relation of eq.(2) with  $L_6 = 3$  and  $\alpha = 3$ , for  $A = 0$  (lower lines) and  $A = 1$  computed at  $z = 1$  (upper lines).

shift interval probed to date. We stress that the high redshift points always lie below or on top of the local relation, with the possible exception of the cluster at  $z = 1.27$ , whose  $X$ –ray spatial distribution suggests this might not be a relaxed system. In general, these data demonstrate that it is reasonable to assume  $A < 1$ , i.e., at most a mild positive evolution of the  $L_{bol}$ – $T_X$  relation.

TABLE 1

Name	Redshift	$L_X (10^{44} \text{ erg s}^{-1})$		$T(\text{keV})$
		EdS	$\Lambda 03$	
RXJ0848+4452 <sup>a</sup>	1.26	$3.03^{+0.83}_{-0.46}$	$5.58^{+1.52}_{-0.85}$	$5.8^{+2.4}_{-1.3}$
RXJ0848+4453 <sup>a</sup>	1.27	$0.63^{+0.25}_{-0.16}$	$1.17^{+0.46}_{-0.29}$	$1.6^{+1.2}_{-0.6}$
RXJ0848+4456 <sup>b</sup>	0.57	$1.13^{+0.34}_{-0.34}$	$1.69^{+0.51}_{-0.51}$	$3.6^{+0.5}_{-0.5}$
CDFS-C11 <sup>c</sup>	0.73	$0.14^{+0.05}_{-0.05}$	$0.22^{+0.09}_{-0.09}$	$1.2^{+0.5}_{-0.4}$
1WGAJ1226.9+3332 <sup>d</sup>	0.89	$45.0^{+4.5}_{-4.5}$	$75.6^{+7.6}_{-7.6}$	$10.5^{+4.0}_{-3.0}$
MS1137.5+6625	0.78	$13.1^{+2.6}_{-2.6}$	$21.3^{+2.6}_{-2.6}$	$5.7^{+0.8}_{-0.6}$
MS1054.4-0321 <sup>e</sup>	0.83	$34.5^{+3.2}_{-3.5}$	$56.9^{+5.3}_{-5.8}$	$10.4^{+1.0}_{-1.0}$

Luminosity and temperature measurements for distant ( $z \geq 0.57$ ) clusters from recent Chandra observations. Column 1: cluster ID (<sup>a</sup> Stanford et al. 2001; <sup>b</sup> Holden et al. 2001; <sup>c</sup> Giacconi et al. 2001, in preparation; <sup>d</sup> Redshift from Ebeling et al. 2001,  $L_X$  and  $T$  from Cagnoni et al. 2001; <sup>e</sup> Jeltema et al. 2001). Column 2: spectroscopic redshift; Columns 3-4: bolometric luminosity, assuming  $h = 0.5$ , for an Einstein–de–Sitter (EdS) cosmology and for a flat low–density model with  $\Omega_m = 0.3$  ( $\Lambda 03$ ). Column 5:  $X$ –ray gas temperature and corresponding  $1\sigma$  uncertainties.

Besides the relevance for the evolution of the mass–luminosity conversion, these results have profound impli-

cations on the physics for the ICM. For instance, the model with constant entropy predicts  $-0.7 < A < 0.7$  depending on the level of the entropy itself and its evolution with cosmic time (Tozzi & Norman 2001). Values of  $A$  in this range are significantly lower than the evolution expected in the self–similar case ( $A = 1.5$ ). Therefore, both the shape and the non–evolution of the  $L_{bol}$ – $T_X$  relation are well explained in models with substantial non–gravitational pre-heating.

In the following we will assume  $\alpha = 3$  and  $A = 0$  as reference values, while we will also show the effect of changing both such parameters. Bolometric and  $K$  corrections to the [0.5–2.0] keV observed band are computed by using a Raymond–Smith (1977) model with  $Z = 0.3$  for the mean ICM metallicity. The global scatter in converting  $X$ –ray luminosity into mass is estimated by adding in quadrature a 15% scatter in the  $M$ – $T_X$  and a 30% scatter in the  $L_{bol}$ – $T_X$  conversion. Its effect is then included in our likelihood analysis by convolving the model luminosity function with a Gaussian function having an r.m.s. scatter of 34%. Finally, for a given  $L_X$ , the flux is computed as  $F = L_X / [4\pi d_L^2(z)]$ .

### 2.3 The analysis method

We apply a maximum–likelihood (ML) approach, to compare the cluster distribution in the flux–redshift,  $(F, z)$ , plane with predictions from a given cosmological model for a sample having the same flux–limit and sky–coverage as the RDCS. As a first step, we divide the  $(F, z)$  plane into elements of size  $dF dz$  and compute the model probability

$$\lambda(F, z) dF dz = n[M(F), z] \frac{dM}{dF} \frac{dV(z)}{dz} f_{sky}(F) dF dz \quad (3)$$

of observing an RDCS cluster with flux  $F$  at redshift  $z$ . Here  $dV(z)$  is the comoving volume element in the redshift interval  $[z, z + dz]$  and  $f_{sky}(F)$  is the RDCS flux-dependent sky-coverage (Rosati et al. 1998). If the bin size is small enough, such probabilities are always much smaller than unity, then the likelihood function  $\mathcal{L}$  of the observed cluster flux and redshift is defined as the product of the Poisson probabilities of observing exactly one cluster in  $dF dz$  at each of the  $(F_i, z_i)$  positions occupied by the RDCS clusters, and of the probabilities of observing zero clusters elsewhere:

$$\mathcal{L} = \prod_i \left[ \lambda(F_i, z_i) dz dF e^{-\lambda(F_i, z_i) dz dF} \right] \prod_{j \neq i} e^{-\lambda(F_j, z_j) dz dF}. \quad (4)$$

Here the indices  $i$  and  $j$  run over the occupied and empty elements of the  $(F, z)$  plane, respectively. If we define the quantity  $S = -2 \ln \mathcal{L}$  and drop all the terms which do not depend on the cosmological model, it is

$$S = -2 \sum_i \ln[\lambda(F_i, z_i)] + 2 \int_0^{z_{max}} dz \int_{F_{lim}}^{\infty} dF \lambda(F, z) \quad (5)$$

(e.g., Marshall et al. 1983). In the above equation,  $z_{max}$  represents the highest redshift at which the cluster identification algorithm, on which RDCS is based, successfully detects extended sources and which, in principle, does not coincide with the highest- $z$  cluster identified in the survey. The  $(1+z)^4$  surface brightness dimming is largely responsible for this high redshift cutoff. Using simulations as those shown in Fig.1 of Rosati et al. (1999), we found  $z_{max} = 1.5$ ; at these redshifts the RDCS sample becomes surface brightness limited for clusters with  $L_X \simeq 10^{44} \text{ erg s}^{-1}$ . We verified that final results are almost left unchanged by taking  $z_{max} = 2$ . Finally, we need to account for non-negligible errors in cluster fluxes, which range from about 5% up to 35%, with a typical value of about 15%. To this purpose, we take clusters not to be defined as points on the  $(F, z)$  plane. Each cluster is spread along the  $F$ -direction using a Gaussian smoothing with r.m.s. amplitude equal to the flux error,  $\epsilon_F$ . Therefore, instead of having zero or unity weight for empty and occupied cells in eq.(5), the  $i$ -th term contributing to the sum is assigned the weight

$$w_i = \sum_m \frac{1}{\sqrt{2\pi\epsilon_{F,m}^2}} \exp \left[ -\frac{(F_m - F_i)^2}{2\epsilon_{F,m}^2} \right] dF, \quad (6)$$

where  $dF$  is its cell flux-width and the sum is over all the clusters having redshift between  $z_i - dz/2$  and  $z_i + dz/2$ .

### 3 RESULTS

We derive constraints on cosmological parameters by searching for the absolute minimum of  $S$  in the three-dimensional  $(\Gamma, \sigma_8, \Omega_m)$  parameter space, and compute confidence regions by allowing for standard increments  $\Delta S$ . Cosmological parameters are varied within the following ranges:  $0.02 \leq \Gamma \leq 0.4$ ,  $0.4 \leq \sigma_8 \leq 1.4$ ,  $0.1 \leq \Omega_m \leq 1$ .

In Figure 3 we show the constraints on the  $(\Omega_m, \sigma_8)$  plane for different values of  $\Gamma$ . As already mentioned, we assume for this reference analysis  $\beta = 1.15$ ,  $L_6 = 3$ ,  $\alpha = 3$  and  $A = 0$ . The most striking result is that the fairly large statistics and the wide  $z$ -baseline provided by RDCS allow stringent constraints to be placed, with  $\Omega_m = 1$  always excluded at much more than the  $3\sigma$  level. The trend toward smaller  $\Omega_m$  for larger  $\Gamma$ s is due to the fact that shallower spectra produce a steeper and more rapidly evolving mass function. Therefore, smaller  $\Omega_m$  values are required to compensate for the more rapid evolution. Although this effect is not large enough to qualitatively affect the resulting constraints, it has nevertheless some effect on the values of the best-fitting parameters. Overall, we obtain the following constraints on the cosmological parameters:

$$\Omega_m = 0.35_{-0.10}^{+0.13} \quad ; \quad \sigma_8 = 0.66_{-0.05}^{+0.06} \quad (7)$$

(errors are  $1\sigma$  confidence levels for three interesting parameters). No significant constraints are found for  $\Gamma$ , meaning that the sampled  $L_X$  range does not correspond to a mass range large enough to probe the shape of the power spectrum. Indeed, RDCS spans about 2.6 decades in  $L_X$ . For the adopted  $M-L_X$  conversion, this corresponds to about 1.3 decades in mass and, therefore, to about 0.4 decades in physical scales. For comparison, constraints on the power-spectrum shape from the galaxy distribution are typically derived by sampling the galaxy clustering over about two decades in physical scales. If we assume  $\Gamma = 0.25$ , as suggested by results from galaxy clustering (e.g., Dodelson & Gaztañaga 2000; cf. also Efstathiou & Moody 2000), then the resulting constraints are  $\Omega_m = 0.28 \pm 0.05$  and  $\sigma_8 = 0.69 \pm 0.06$ , where errors are now for two significant parameters. By assuming instead open geometry with vanishing cosmological constant, this constraint changes into  $\Omega_m = 0.35 \pm 0.06$  and  $\sigma_8 = 0.60 \pm 0.03$ . This shows the tendency of flat models to favor slightly smaller values of  $\Omega_m$ , as a consequence of the larger linear perturbation growth rate in the presence of a cosmological constant term.

Also shown in Fig. 3 are the model predictions for the number of clusters expected in RDCS-1. The different curves in each panel show the *loci* of the  $\Omega_m$ - $\sigma_8$  plane corresponding to a fixed number of RDCS clusters expected at  $z > 0.9$  and  $F > 1 \times 10^{-14} \text{ erg s}^{-1} \text{ cm}^{-2}$ . Quite remarkably, the four clusters detected in RDCS-1 can always be produced by cosmological models which lie inside the  $1\sigma$  contours defined by the RDCS-3. On the one hand, this result implies that the XLF evolution traced by brighter clusters at  $z \lesssim 0.85$  also extends at fainter fluxes out to the highest redshift reached by RDCS. On the other hand, it suggests that RDCS is not significantly affected by incompleteness or unaccounted systematics also at fluxes  $10^{-14} \text{ erg s}^{-1} \text{ cm}^{-2} < F_X < 3 \times 10^{-14} \text{ erg s}^{-1} \text{ cm}^{-2}$ . It should be said, however, that given the relatively small survey volume at these low fluxes, such systematics have in general a small impact on observed distribution functions.

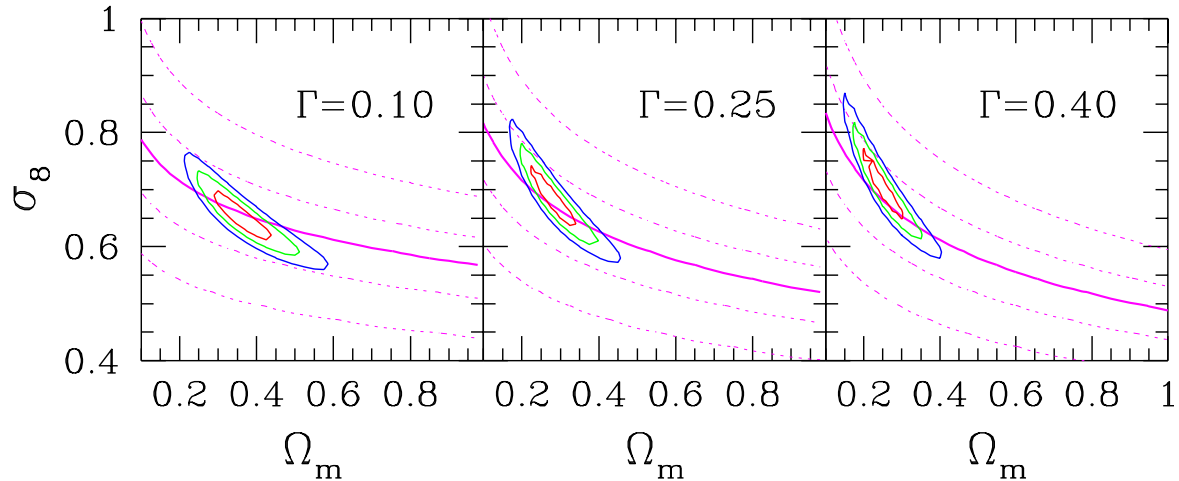


Fig. 3.— Confidence regions on the  $\Omega_m$ - $\sigma_8$  plane for different choices of the power-spectrum shape-parameter  $\Gamma$ . Here  $\alpha = 3$ ,  $A = 0$  and  $\beta = 1.15$  have been assumed for the mass-luminosity conversion. Contours are  $1\sigma$ ,  $2\sigma$  and  $3\sigma$  c.l. for two interesting parameters. The dotted curves show the the  $\Omega_m$ - $\sigma_8$  relations corresponding to a given number of clusters,  $N_c$ , expected in RDCS-1 at  $z \geq 0.9$ ;  $N_c = 0.1, 1, 10, 30$  from lower to upper curve. The solid curve correspond to the actually observed 4 clusters.

In Fig. 4 we show the effect of changing in different ways the mass-luminosity conversion, after fixing  $\Gamma = 0.25$ . The main result from these tests is that  $\Omega_m < 0.6$  at least at the  $3\sigma$  c.l. for any variation of the mass-luminosity conversion within realistic observational and theoretical uncertainties. Looking at the details of the effects, a positive evolution of the  $L_{bol}$ - $T_X$  relation, which is only marginally allowed by data (e.g., Donahue et al. 1999; Della Ceca et al. 2000; Fairley et al. 2000; see also Fig. 2), turns into smaller masses of more distant clusters for a fixed  $L_X$ . This increases the amount of evolution inferred for the mass function and allows for a slightly larger  $\Omega_m$ . A shallower slope of the local  $L_{bol}$ - $T_X$  relation provides relatively smaller masses for less luminous clusters. Since low  $L_X$  objects are sampled at low redshift, this has the effect of decreasing the amplitude of the mass function at low  $z$ , so as to decrease its evolution, thus implying a lower  $\Omega_m$ . We have also verified that the observed steepening at the scale of galaxy groups (e.g., Helsdon & Ponman 2000) has negligible effect on our results, only a few intermediate- $z$  RDCS clusters being faint enough to be classified as groups. Finally, a larger  $\beta$  implies a larger cluster mass for a fixed  $T_X$ , so that a larger  $\sigma_8$  is required to match the amplitude of the cluster XLF. In turn, a larger  $\sigma_8$  slows down the evolution of the model mass function, thus allowing for a larger  $\Omega_m$ .

These constraints on  $\Omega_m$  are consistent with those found from some analyses of the XTF evolution. Eke et al. (1998) combined the temperature data for 25 local clusters by Henry & Arnaud (1991) with the sample of 10 EMSS clusters at  $0.3 < z < 0.4$  by Henry (1997) and found  $\Omega_m \simeq 0.40 \pm 0.25$  at the  $1\sigma$  c.l. Donahue & Voit (1999) used the low- $z$  sample by Markevitch (1998) and enlarged the high- $z$  sample by adding further 5 clusters at  $0.50 \leq z \leq 0.83$ ; for flat geometry, they constrained the density parameter to lie in the range  $\Omega_m \simeq 0.3 \pm 0.1$  at the  $1\sigma$  c.l. Henry (2000) combined the low- $z$  data by Henry

& Arnaud (1991) with ASCA temperatures for 15 EMSS clusters at  $0.3 < z < 0.6$ , and found  $\Omega_m = 0.44 \pm 0.12$  at the  $1\sigma$  c.l. for one fitting parameter, in the case of flat geometry.

As already mentioned, such constraints from the XTF could be weakened by the lack of a homogeneous sample of cluster temperatures selected at low and high redshift. For instance, Viana & Liddle (1999) used the same data set as Eke et al. (1998) and showed that uncertainties both in fitting local data and in the theoretical modelling could significantly change final results. They found  $\Omega_m \simeq 0.75$  as a preferred value, with a critical-density model acceptable at  $< 90\%$  c.l. Blanchard et al. (2000) derived a local XTF for clusters from the XBACs (Ebeling et al. 1996). The higher power-spectrum normalization they derived from this sample turned into a slower XTF evolution and, therefore, a higher  $\Omega_m$ . As a result, they derived  $\Omega_m \simeq 0.9 \pm 0.3$  at the  $1\sigma$  c.l. We stress here that the possible ambiguity connected with the choice of the low- $z$  sample and the combination of different data sets at different redshift ranges is not an issue in our analysis, owing to the uniform selection provided by the RDCS over its entire redshift range.

Besides the RDCS, the EMSS is the only other X-ray flux-limited sample that has been used to date to derive cosmological constraints. Sadat et al. (1988) used the EMSS redshift distribution, while Reichart et al. (1999) followed the evolution of the  $L_X$  distribution. After using a slowly evolving  $L_X$ - $T$  relation, they found  $\Omega_m$  to be consistent with unity and, therefore, significantly higher than the values preferred by our RDCS analysis.

As for the amplitude of the power spectrum, our best fitting value of  $\sigma_8$  is somewhat smaller than those indicated by other analyses. For instance, fixing  $\Gamma = 0.25$  and  $\Omega_m = 0.3$ , we find from the reference analysis shown in Fig. 3 that  $\sigma_8 = 0.67 \pm 0.06$  at the  $3\sigma$  c.l. for one interesting parameter, while Eke et al. (1998) find  $\sigma_8 \simeq 0.8$

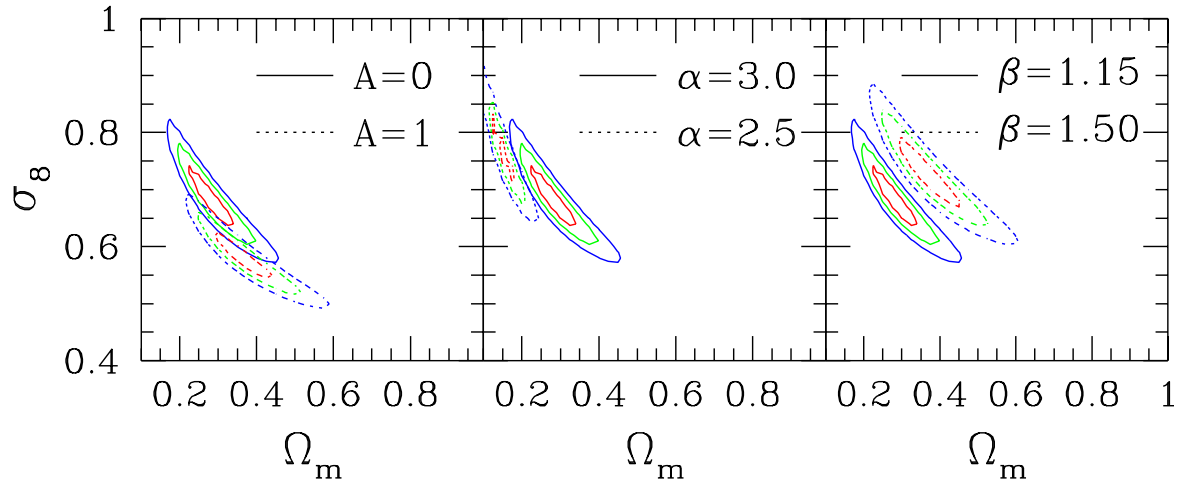


Fig. 4.— Effect of changing the mass–luminosity relation. Solid contours are from assuming  $\Gamma = 0.25$ ,  $\alpha = 3$ ,  $A = 0$  and  $\beta = 1.15$ . Each panel corresponds to changing one of the parameters defining the mass–luminosity relation. Contours have the same meaning as in Fig. 3.

with about 20% uncertainty. We verified that this difference can be partly explained by the fact that we used here the mass function by Sheth & Tormen (1999). At the effective mass scale probed by RDCS this mass function is somewhat larger than that by Press & Schechter (1974), thus requiring a lower power–spectrum normalization to match data. We repeated our analysis with the standard Press–Schechter recipe and found  $\sigma_8 = 0.72$  for the same choice of  $\Omega_m$  and  $\Gamma$ . Furthermore, we verified that, for the same parameter choice, increasing  $\beta$  to 1.25 is enough to increase  $\sigma_8$  by a further 10%.

Finally, we point out that the constraints obtained with the present analysis are more stringent than those we derived in BRTN. In that paper we used the XLF, binned in luminosity and redshift, for a smaller version of the RDCS, and found constraints on  $\Omega_m$  which were quite dependent on the assumed evolution of the  $L_X$ – $T$  relation. Assuming non–evolution for this relation, we derived  $\Omega_m \simeq 0.4 \pm 0.3$  at the 90% c.l. for flat models. The much more stringent constraints derived in the present analysis are due to two main reasons: the larger number of clusters in the RDCS, extending to higher redshifts and fainter fluxes; and the new analysis which extracts more information than was previously possible with a simple grouping of RDCS clusters into luminosity and redshift intervals. Indeed, the likelihood function defined by eq.(5) conveys all the information provided by the cluster distribution within the portion of the  $(F, z)$  plane accessible to RDCS.

#### 4 CONCLUSIONS

In this paper we analyzed the evolution of the cluster number density, as traced by the ROSAT Deep Cluster Survey (RDCS, Rosati et al. 1998, 2000) out to  $z \simeq 1.3$ , to derive constraints on the  $\Omega_m$  and  $\sigma_8$  cosmological parameters. Our analysis was aimed at understanding whether uncertainties in the relation between cluster mass,  $M$ , and X–ray luminosity,  $L_X$ , prevent us from drawing firm con-

clusions. In principle, a major source of uncertainty is related to the evolution of the  $M$ – $T_X$ – $L_X$  relation. The most recent data shown in Fig. 2 allow us now to trace the  $L_{bol}$ – $T_X$  relation out to  $z \simeq 1.3$  (Stanford et al. 2001), without evidence of significant evolution. This result also agrees with predictions from semi–analytical models of the ICM aimed at explaining the excess entropy observed in cluster cores (e.g., Tozzi & Norman 2001, and references therein). These findings are now significantly reducing the uncertainties on the evolution of the X–ray properties of cluster.

As a main result we find that, within both theoretical and observational uncertainties in the  $M$ – $L_X$  relation, the density parameter is always constrained to lie in the range  $0.1 \lesssim \Omega_m \lesssim 0.6$  at the  $3\sigma$  c.l. This demonstrates that X–ray luminosities as a function of redshift from deep X–ray flux–limited cluster surveys are indeed powerful tools to probe cosmological scenarios.

Serendipitous cluster searches with Chandra and XMM–Newton archival data will lead to larger distant cluster samples within the next few years, and provide temperature information for a substantial number of objects. Flux–limited surveys will open the way to quantify the evolution of the cluster XLF with unprecedented accuracy, while the availability of many more cluster temperatures, even for incomplete samples, will provide a precise calibration of the  $L_{bol}$ – $T_X$  relation and its evolution.

With this perspective, the main limitation to further tightening constraints on cosmological parameters will come from our theoretical understanding of what a cluster actually is. While we benefited from the recent results on the thermodynamics of the ICM for the present analysis, another significant source of uncertainty stems from the dynamical aspects of clusters of galaxies. For instance, the limited validity of the assumptions on which the relation between X–ray temperature and virial mass is based (e.g., spherical collapse and hydrostatic equilibrium, see Voit 2000), makes the connection with model predictions



somewhat uncertain. Furthermore, as observations are reaching the first epoch of cluster assembly, treating them as dynamically relaxed and virialized systems is undoubtedly an oversimplification. In fact, hierarchical clustering scenario predicts that a fraction, between 0.3 and 0.6, of the  $z = 1$  population of groups and clusters are observed less than 1 Gyr after the last major merger event and, therefore, are likely to be in a state of non-equilibrium.

Although such uncertainties have been so far of minor importance with respect to the paucity of observational data, a breakthrough is however needed in the quality of the theoretical framework if high-redshift clusters are to take part in the high-precision era of observational cosmology. In this respect, hydrodynamical cluster simulations designed to include all the relevant ICM physics will play a fundamental role in the years to come.

We thank the anonymous referee for his/her detailed review of the paper. SB wish to thank ESO in Garch-

ing for the hospitality during several phases in the preparation of this work. We also thank T. Jeltema for providing us with  $L_X$  and  $T$  for MS1054, from their analysis of Chandra data, in advance of publication. Support for SAS came from NASA/LTSA grant NAG5-8430 and for BH from NASA/Chandra GO0-1082A, and both are supported by the Institute of Geophysics and Planetary Physics (operated under the auspices of the US Department of Energy by the University of California Lawrence Livermore National Laboratory under contract W-7405-Eng-48). Portions of this work were carried out by the Jet Propulsion Laboratory, Californian Institute of Technology, under a contract with NASA. Support for this work was also provided by NASA through Hubble Fellowship Grant No. HF-01114.01-98A from the Space Telescope Science Institute, which is operated by the Association of Universities for Research in Astronomy, Incorporated, under NASA Contract NAS5-26555.

## REFERENCES

- Allen, S.W., & Fabian, A.C. 1998, MNRAS, 297, L57  
 Arnaud, M., & Evrard, A.E. 1999, MNRAS, 305, 631  
 Bardeen, J.M., Bond, J.R., Kaiser, N., & Szalay, A.S. 1986, ApJ, 304, 15  
 Blanchard, A., Sadat, R., Bartlett, J.G., & Le Dour, M. 2000, A&A, 362, 809  
 Borgani, S., Rosati, P., Tozzi, P., & Norman, C. 1999, ApJ, 517, 40 (BRTN)  
 Borgani, S., Girardi, M., Carlberg, R.G., Yee, H.K.C., & Ellingson, E. 1999b, ApJ, 527, 561  
 Borgani, S., & Guzzo, L. 2001, Nature, 409, 39  
 Bryan, G.K., & Norman M.L. 1998, ApJ, 495, 80  
 Cagnoni, I., Elvis, M., Kim, D.-W., Mazzotta, P., Huang, J.-S., & Celotti, A. 2001, ApJL, in press  
 Carlberg, R.G., Yee, H.K.C., & Ellingson, E. 1997, ApJ, 478, 462  
 Colafrancesco, S., Mazzotta, P., & Vittorio, N. 1997, ApJ, 488, 566  
 de Bernardis, P., et al. 2000, Nature, 404, 955  
 Della Ceca, R., Scaramella, R., Gioia, I.M., Rosati, P., Fiore, F., & Squires, G. 2000, A&A, 353, 498  
 Dodelson, S., & Gaztañaga, E. 2000, MNRAS, 312, 774  
 Donahue, M., & Voit, G.M. 1999, ApJ, 523, L137  
 Donahue, M., Voit, G.M., Scharf, C.A., Gioia, I.M., Mullis, C.R., Hughes, J.P., & Stocke, J.T. 1999, ApJ, 527, 525  
 Ebeling, H., Voges, W., Böhringer, H., et al. 1996, MNRAS, 281, 799  
 Ebeling, H., Jones, L.R., Fairley, B.W., Perlman, E., Scharf, C., & Horner, D. 2001, ApJ, 584, L23  
 Eke, V.R., Cole, S., Frenk, C.S., & Henry, J.P. 1998, MNRAS, 298, 1145  
 Efstathiou, G., & Moody, S.J. 2000, MNRAS, submitted (astro-ph/0010478)  
 Evrard, A.E., MacFarland, T.J., Couchman, H.M.P., et al. (The Virgo Consortium) 2001, ApJ, submitted  
 Evrard, A.E., Metzler, C.A., & Navarro, J.F. 1996, ApJ, 469, 494  
 Fairley, B.W., Jones, L.R., Scharf, C., Ebeling, H., Perlman, E., Horner, D., Wegner, G., & Malkan, M. 2000, MNRAS, 315, 669  
 Finoguenov, A., Reiprich, T.H., & Böhringer, H. 2001, A&A, 368, 749  
 Frenk, C.S., et al. 2000, ApJ, 525, 554  
 Giacconi, R., Rosati, P., Tozzi, P., et al. 2001, ApJ, 551, 624  
 Gioia, I.M., Henry, H.P., Maccacaro, T., Morris, S.L., Stocke, J.T., & Walter, A. 1990, ApJ, 356, L35  
 Gioia, I.M., Henry, J.P., Mullis, C.R., Voges, W., Briel, U.G., Böhringer, H., & Huchra, J.P. 2001, ApJ, 553, L109  
 Gioia, I.M. 2000, in "Constructing The Universe With Clusters Of Galaxies", Paris, France (astro-ph/0010059)  
 Girardi, M., Borgani, S., Giuricin, G., Mardirossian, F., & Mezzetti, M. 1998, ApJ, 506, 45  
 Governato, F., Babul, A., Quinn, T., Tozzi, P., Baugh, C. M., Katz, N., & Lake, G. 1999, MNRAS, 307, 949  
 Hanany, S., et al. 2000, ApJ, 545, L5  
 Helsdon, S.F., & Ponman, T.J. 2000, MNRAS, 315, 356  
 Henry, J.P., 1997, ApJ, 489, L1  
 Henry, J.P., 2000, ApJ, 534, 565  
 Henry, J.P., & Arnaud, K.A. 1991, ApJ, 1991, 372, 410  
 Henry, J.P., Gioia, I.M., Maccacaro, T., Morris, S.L., Stocke, J.T., & Wolter A. 1992, ApJ, 386, 408  
 Holden, B.P., Stanford, S.A., Rosati, P., Squires, G., Tozzi, P., Fosbury, R.A.E., & Papovich, C. 2001, ApJL, in press  
 Kitayama, T., & Suto, Y. 1997, ApJ, 490, 557  
 Jeltema, T.E., Canizares, C.R., Bautz, M.W., Malm, M.R., Donahue, M., & Garmire, G.P. 2001, ApJ, submitted  
 Jenkins, A., Frenk, C.S., White, S.D.M., Colberg, J., Cole, S., Evrard, A.E., & Yoshida, N. 2001, MNRAS, 321, 372  
 Jones, L.R., Scharf, C., Ebeling, H., Perlman, E., Wegner, G., Malkan, M., & Horner, D. 1998, ApJ, 495, 100  
 Markevitch, M. 1998, ApJ, 504, 27  
 Marshall, H.L., Avni, Y., Tananbaum, H., & Zamorani, G. 1983, ApJ, 269, 35  
 Mathiesen, B., & Evrard, A.E. 1998, MNRAS, 295, 769  
 Metzler, C., Evrard, A.E., & Navarro, J.F. 1006, ApJ, 469, 494  
 Mushotzky, R.F., & Scharf, C.A. 1997, ApJ, 482, L13  
 Oukbir, J., & Blanchard, A. 1992, A&A, 262, L21  
 Pierpaoli, E., Scott, D., & White, M. 2001, MNRAS, 325, 77  
 Ponman, T. J., Cannon, D. B., & Navarro, F.J. 1999, Nature, 397, 135  
 Press, W.H., & Schechter, P. 1974, ApJ, 187, 425  
 Reichart, D.E., Nichol, R.C., Castander, F.J., Burke, D.J., Romer, A.K., Holden, B.P., Collins, C.A., & Ulmer, M.P. 1999, ApJ, 518, 521  
 Raymond, J.C., & Smith, B.W. 1977, ApJS, 35, 419  
 Romer, A.K., et al. 2000, ApJS, 126, 209  
 Rosati, P., Borgani, S., Della Ceca, R., Stanford, S.A., Eisenhardt, P.R., & Lidman, C. 2000, in "Large Scale Structure in the X-ray Universe", Santorini, Greece, p.13  
 Rosati, P., Della Ceca, R., Burg, R., Norman, C., & Giacconi, R., 1995, ApJ, 445, L11  
 Rosati, P., Della Ceca, R., Burg, R., Norman, C., & Giacconi, R., 1998, ApJ, 492, L21  
 Rosati, P., Stanford, S.A., Eisenhardt, P.R., Elston, R., Spinrad, H., Stern, D. & Dey, A. 1999, AJ, 118, 76  
 Sadat, R., Blanchard, A., & Oukbir, J. 1998, A&A, 329, 21

- Sheth, R.K., & Tormen, G. 1999, MNRAS, 308, 119  
Stanford, S.A., Rosati, P., Holden, B., Tozzi, P., Borgani, S., Eisenhardt, P.R., & Spinrad, H. 2001, ApJ, 552, 504  
Tozzi, P., Rosati, P., Nonino, M., et al. 2001, ApJ, in press (astro-ph/0103014)  
Tozzi, P., & Norman, C. 2001, ApJ, 546, 63  
Viana, P.T.P., & Liddle, A.R. 1999, MNRAS, 303, 535  
Vikhlinin, A., McNamara, B.R., Forman, W., Jones, C., Quintana, H., & Hornstrup, A. 1998, ApJ, 502, 558  
Voit, G.M. 2000, ApJ, 545, 670  
White, D.A., Jones, C., & Forman, W. 1997, MNRAS, 292, 419  
White, S.D.M., Efstathiou, G., & Frenk, C.S. 1993, MNRAS, 262, 1023  
Wu, X.-P., Xue, Y.-J., & Fang, L.-Z. 1999, ApJ, 524, 22